Influence of Titanium in Nickel-Base Superalloys on the Performance of Thermal Barrier Coatings Utilizing $\gamma-\gamma'$ Platinum Bond Coats

H. M. Tawancy

Luai M. Al-Hadhrami

Center for Engineering Research and Center of
Research Excellence in Corrosion,
Research Institute,
King Fahd University of Petroleum and Minerals,
P.O. Box 1639,
Dhahran 31261, Saudi Arabia

Titanium is a key element in nickel-base superalloys needed with aluminum to achieve the desired volume fraction of the strengthening γ'-phase. However, depending upon its concentration, titanium can degrade the adherence of aluminum oxide by forming TiO_2 particles near the oxide-metal interface. This effect is extended to thermal barrier coating systems where in this case, the bond coat replaces the superalloy as the underlying substrate. Noting that the onset of failure of thermal barrier coating systems coincides with the first spall of the thermally grown oxide, titanium level in the superalloy can have an important effect on the useful life of the coating. Therefore, this study was undertaken to examine the effect of titanium on the performance of a thermal barrier coating system. Included in the study were two Ni-base superalloys with similar chemical composition except for the Ti content and a Pt-containing bond coat consisting of $\gamma' + \gamma$-phases all top coated with zirconia stabilized by 7 wt % yttria. Coating performance was evaluated from thermal exposure tests at $1150\,^{\circ}C$ with a 24 h cycling period to room temperature. Various electron-optical techniques were used to characterize the microstructure. The coating system on the low-Ti alloy was found to outperform that on the high-Ti alloy. However, for both alloys, failure was observed to occur by loss of adhesion between the thermally grown oxide and underlying bond coat. [DOI: 10.1115/1.4002154]

1 Introduction

Several studies have demonstrated that the adhesion between thermally grown oxide and underlying bond coat plays an important role in limiting the useful life of thermal barrier coating systems, e.g., Ref. [1]. Therefore, there is a considerable interest in developing bond coats highly resistant to oxidation. Toward this objective, it is essential to establish a better understanding of the coating degradation modes, which influence the integrity of the thermally grown oxide and in turn limits the service life of the component. In this regard, the composition of superalloy substrates can be a limiting factor requiring bond coats particularly those of the diffusion-type to be tailored for specific alloys. Information generated from such studies, however, can significantly contribute to improving the performance of existing coating systems and/or developing new coatings of more universal applicability.

Superalloys used in gas turbine blade applications contain various concentrations of Ti, which is added to enhance the properties of the strengthening γ'-phase. However, depending upon its concentration, Ti can degrade the adherence of Al_2O_3 scale by forming TiO_2 particles near the oxide-metal interface [2,3]. Among the various bond coats of the diffusion-type, which can reduce the detrimental effect of Ti is a modified version of Pt-aluminides consisting of a mixture of $\gamma' + \gamma$ phases [4–7]. Incorporation of Pt into the γ'-phase is found to promote its thermal stability, which could increase its effectiveness as a sink for Ti [8–10].

To better understand the role of Ti, this study was undertaken to determine the effect of its concentration in the superalloy substrate on the overall coating performance. Two single-crystal superalloys of about the same composition with the exception of Ti were selected for the study. For both alloys, the coating system had the same thickness and composition (top coat: zirconia +8 wt % yttria, bond coat: Pt-rich $\gamma' + \gamma$).

2 Procedure

Table 1 shows the nominal chemical compositions of the alloys used in the study. Samples were in the form of rods about 10 cm in length and 8 mm in diameter. The bond coat was applied on the grit-blasted alloy surface by electroplating a layer of Pt about 10 μm in thickness. A diffusion/pre-oxidation heat treatment for 4 h at $1150\,^{\circ}C$ in air was used to develop: (1) the bond coat microstructure and (2) a thin surface layer of Al_2O_3 about 1 μm in thickness to enhance the adhesion of the ceramic top coat. Subsequently, a layer of the top coat (ZrO_2+8 wt % Y_2O_3) about 250 μm in thickness was deposited using the technique of electron-beam physical vapor deposition (EB-PVD) [11]. In the as-deposited condition, the thickness of the bond coat was about 40 μm. Thermal exposure tests in air at $1150\,^{\circ}C$ with a 24 h cycling period to room temperature were used to: (1) determine the relative performance of the coating system on the two superalloy substrates listed in Table 1 and (2) characterize the thermal stability characteristics and thickening rate of the thermally grown oxide. All samples were air-cooled. Scanning electron microscopy, electron-probe microanalysis, and X-ray diffraction were used to characterize the microstructures.

3 Results and Discussion

3.1 Coating Performance. Figure 1 shows an example derived from the high-Ti alloy 1 (Table 1) to illustrate characteristic microstructural features of the coating system. As shown in Fig.

Table 1 Nominal chemical compositions of the alloys included in the study (wt %)

Element	Ni	Co	Cr	Al	Ti	Ta	W	Re	Mo	Hf
High-Ti alloy 1	Bal.	9.5	6.2	5.5	1.0	6.5	6.5	2.9	0.6	0.1
Low-Ti alloy 2	Bal.	9.5	6.2	5.5	0.3	8.5	6.5	2.9	0.6	0.1

1(a), the top ceramic coat with an average thickness of about 250 μm had the characteristic columnar grain structure typically produced by EB-PVD. The bond coat with a total average thickness of about 40 μm can be seen to be separated from the top coat by a thin layer of Al_2O_3 about 1 μm in thickness. As shown in the example of Fig. 1(b), the bond coat consisted of three distinct zones: (1) an outermost massive layer of Pt-rich γ'-phase containing small islands of γ-phase (zone 1), (2) an intermediate layer consisting of a mixture of lamellar γ'-phase with less Pt content in a matrix of γ-phase (zone 2), and (3) an inner layer of alloy-depleted zone (zone 3).

Detailed microchemical analysis indicated that the composition of the outermost layer of γ'-phase was predominantly of the type $(Ni, Pt, Cr)_3(Al, Ti, Pt)$ noting that Pt could replace for both Ni and Al [12,13]. However, the γ'-phase observed within the inner layer contained less Pt and higher concentrations of transition metals particularly Ta, which could explain the observed lamellar morphology related to the $\gamma' - \gamma$ lattice mismatch. Alloy substrate elements transported into the bond coat during its formation could lead to the creation of the observed alloy-depleted zone. Similar results were obtained in the case of the low-Ti alloy 2.

The coating system on the low-Ti alloy 2 was observed to outperform that on the high-Ti alloy 1 as demonstrated in Fig. 2(a). Failure of the coating system was indicated by macroscopic spallation of the top coat. Consistent with this result, localized decohesion between the thermally grown oxide and bond coat was observed in the case of alloy 1 during the earlier stages of thermal exposure as shown in Figs. 2(b) and 2(c). It is to be noted from this example that for both alloys, the thickness of the oxide layer

was about the same after 120 h of exposure suggesting that the stresses generated by the thermally grown oxide had very little or no effect on the relative performance of the coating system on the two alloys. This is further confirmed by the comparative thickening rate of the thermally grown oxide shown in Fig. 3. It is evident that both alloys exhibited a similar behavior in that the bond coat was able to develop a protective oxide scale as indicated by the primary oxidation stage followed by a steady state. Although Ti can also increase the growth rate of Al_2O_3 [2,3], it is likely that formation of less protective oxides due to interdiffusion with the alloy substrate could have significantly contributed to the observed accelerated oxidation rate toward the end of the coating life. However, the onset of this stage during the earlier stages of thermal exposure in the case of alloy 1, could be related to its higher Ti content as shown later.

3.2 Thermal Stability Characteristics. Observations of the coarsening of g'-phase with thermal exposure time at 1150°C showed that the bond coat on the two alloys exhibited similar thermal stability characteristics. Figure 4 shows an example derived from alloy 1 to illustrate typical microstructural characteristics along a cross section of the bond coat as a function of exposure time at 1150°C. As can be seen, substantial coarsening of the γ'-phase occurred with continued thermal exposure. This was associated with outward diffusion of Ni and other substrate elements and inward diffusion of Pt. For example, Figs. 5 and 6 show the effect of exposure time at 1150°C on the concentrations of Pt and Ni in the bond coat on alloys 1 and 2, respectively.
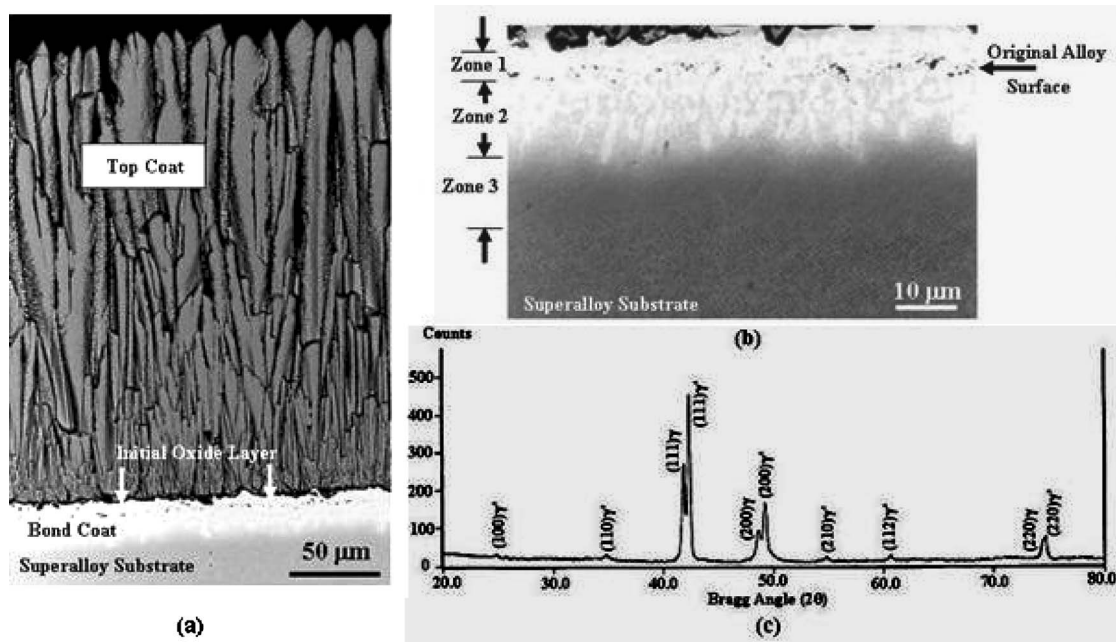
Fig. 1 An example derived from alloy 1 to illustrate characteristic microstructural features of the coating system in the as-deposited condition: (a) backscattered electron image along a cross section of the coating and into the alloy substrate showing the gross microstructural features, (b) backscattered electron image showing typical microstructural features of the bond coat, and (c) an X-ray diffraction pattern derived from the surface of the bond coat
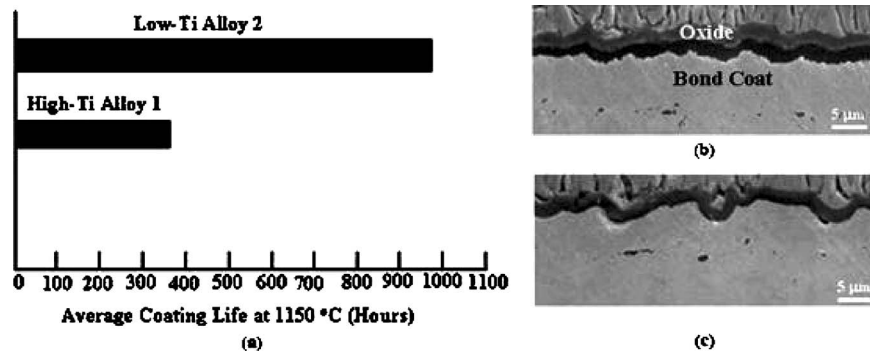
Fig. 2 Comparative performance of the coating system on the two alloys included in the study as determined from thermal exposure tests at 1150°C with a 24 h cycling period to room temperature: (*a*) average coating life, (*b*) secondary electron image along a cross section of the bond coat on alloy 1 after 120 h of exposure at 1150°C showing localized decohesion between the bond coat and thermally grown oxide, and (*c*) secondary electron image along a cross section of the bond coat on alloy 2 after 120 h of exposure at 1150°C; although the oxide thickness was about the same as for alloy 1, good adherence to the bond coat was still maintained
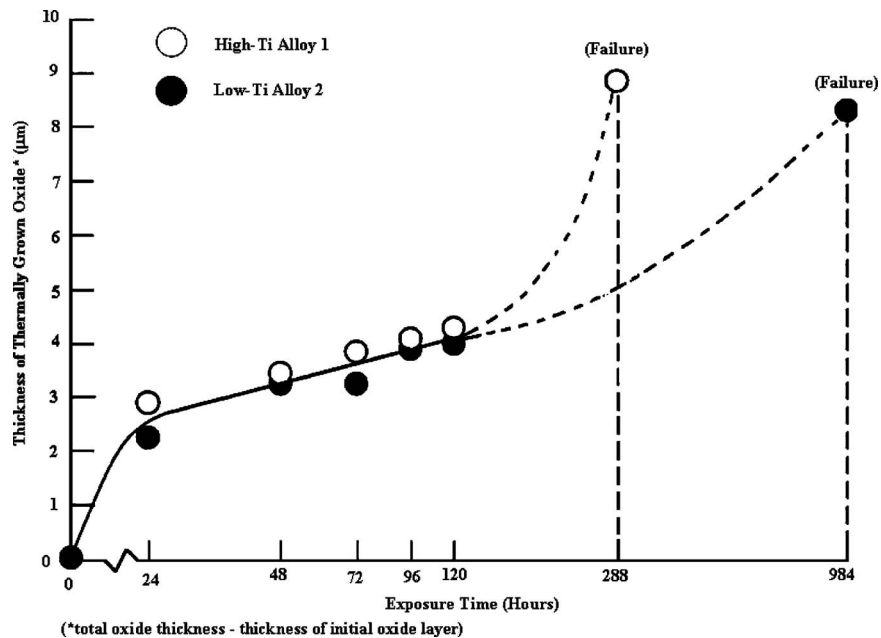
Fig. 3 Comparative thickening rate of the thermally grown oxide during thermal exposure at 1150°C in air with a 24 h cycling period to room temperature
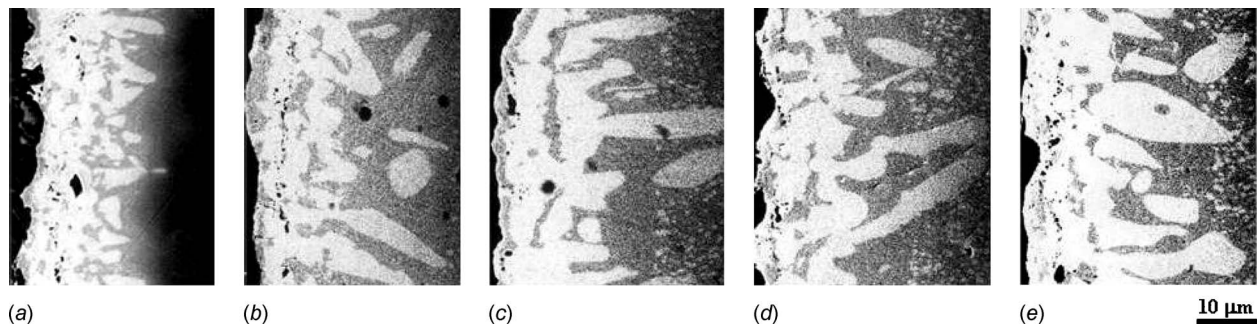
Fig. 4 An example derived from alloy 1 to illustrate the thermal stability of the bond coat during thermal exposure at 1150°C. (*a*)–(*e*) Backscattered electron images along a cross section of the bond coat: (*a*) as-deposited condition, (*b*) 24 h of exposure, (*c*) 48 h of exposure and 72 h of exposure, (*d*) 96 h of exposure, and (*e*) 120 h of exposure.
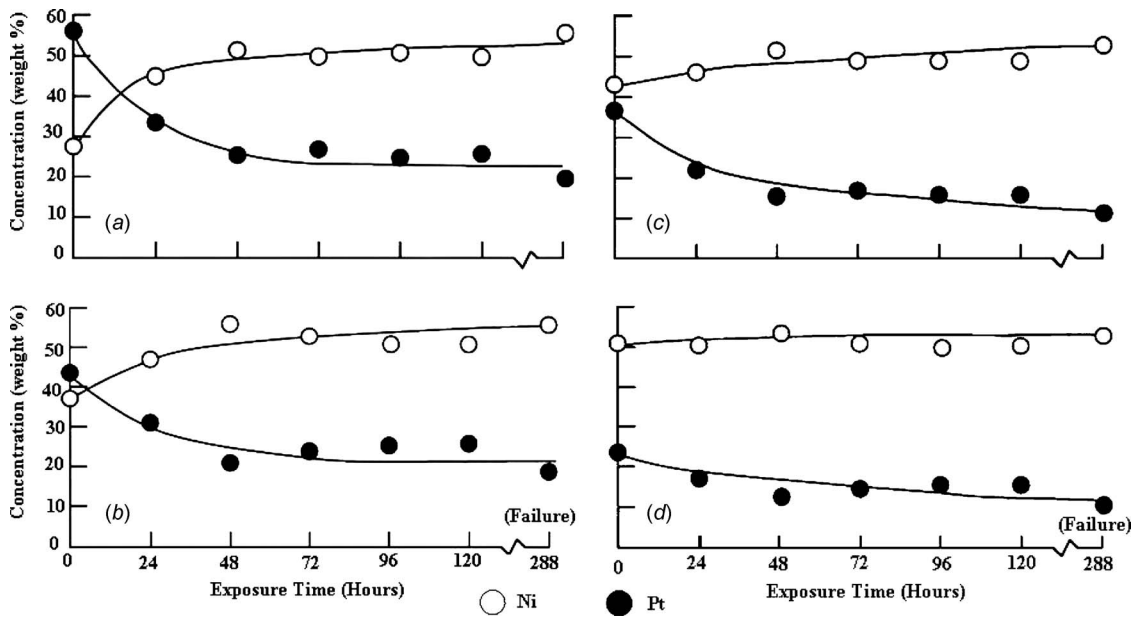
Fig. 5 Effect of exposure time at 1150°C on the concentrations of Pt and Ni in the bond coat on alloy 1: (*a*) surface layer of γ'-phase, (*b*) inner layer of γ'-phase, (*c*) γ-phase near the surface, and (*d*) inner layer of γ-phase

Inward diffusion of Pt and outward diffusion of Ni, as shown in Figs. 5 and 6, would be expected to lower the thermal stability of the γ'-phase releasing Ti, which could degrade the adherence of the thermally grown oxide. The corresponding effect on Ti concentration within the surface layers of γ'- and γ-phases is shown in Fig. 7. It is observed that after a given exposure time, the concentration of Ti in the surface layers of γ-phase in the high-Ti alloy 1 was $\geq$10 times that corresponding to the low-Ti alloy 2.

3.3 Failure Mechanism of the Coating System. Detailed microstructural characterization showed that for both alloys, failure of the coating system occurred by decohesion between the thermally grown oxide and underlying bond coat. Therefore, the

above results suggested the difference in behavior between the two alloys could be related to the dynamics of the process leading to spallation of the thermally grown oxide.

Figure 8 shows a typical example illustrating the microstructural features of the surfaces exposed by failure of the coating system. The exposed surface of the top coat was covered by a layer of Al_2O_3 containing various concentrations of substrate elements. As shown in Fig. 8(*a*), the oxide layer exhibited a web-type appearance typical of Al_2O_3. Figure 8(*b*) shows the corresponding surface of the bond coat, which was found to predominantly consist of γ-phase. Debris of the ceramic top coat exhibiting black contrast could be distinguished at the surface of the bond coat. At
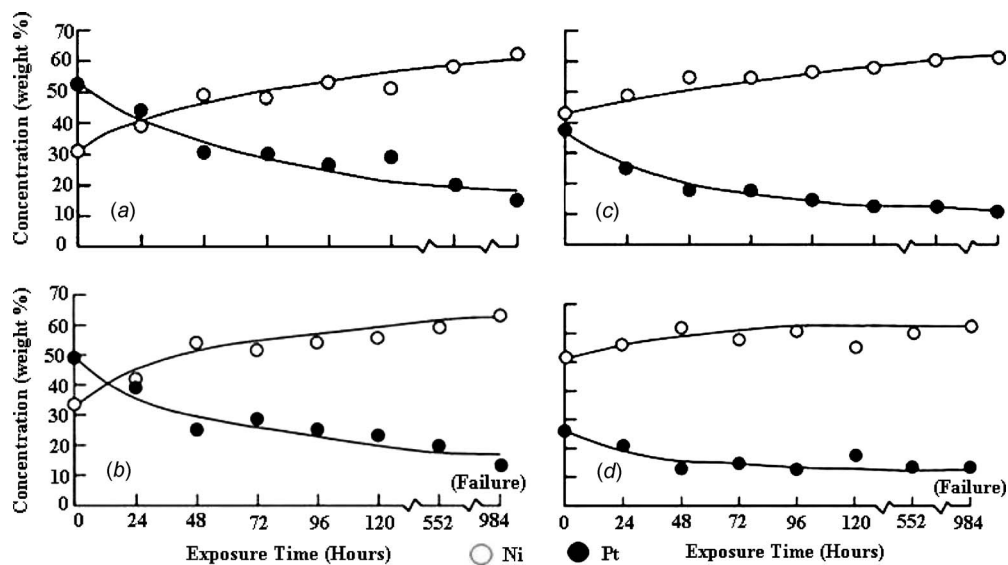
Fig. 6 Effect of exposure time at 1150°C on the concentrations of Pt and Ni in the bond coat on alloy 2: (*a*) surface layer of γ'-phase, (*b*) inner layer of γ'-phase, (*c*) γ-phase near the surface, and (*d*) Inner layer of γ-phase
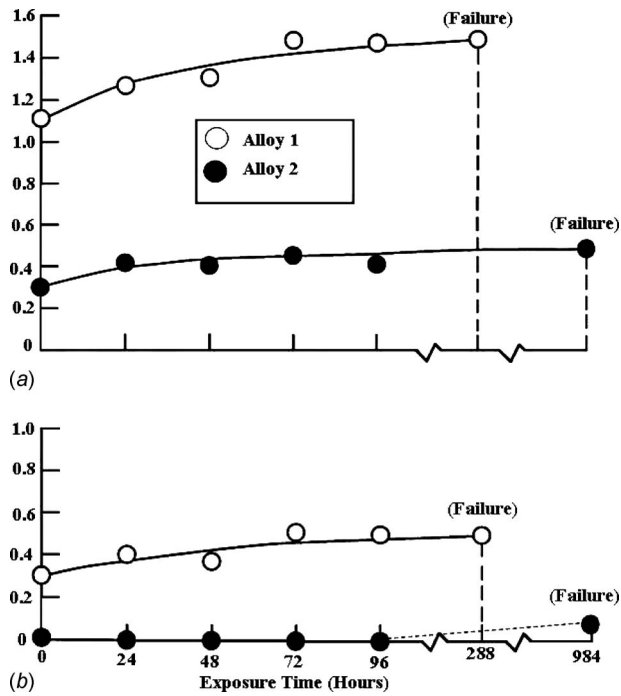
Fig. 7 Effect of exposure time at 1150°C on the Ti concentration in the bond coat on alloys 1 and 2: (*a*) surface layer of γ'-phase, and (*b*) γ-phase near the surface

higher magnifications, both the bond coat and top coat surfaces were found to contain small voids with an average diameter of about 1 μm or less as shown in the example of Fig. 8(*c*). Particles of Ti-rich oxide could be identified within some of these voids as shown in the corresponding X-ray spectrum of Fig. 8(*d*). These results are consistent with the significant increase in Ti concentration observed in Fig. 7(*b*) indicating that formation of Ti-rich oxide near the bond coat surface had an adverse effect on the adhesion of the thermally grown oxide as described below.

It could be concluded from the above observations that spallation of the thermally grown oxide was facilitated by forming Ti-rich oxide particles expected to be TiO_2 near the oxide-bond coat interface as schematically illustrated in Fig. 9. Localized stress concentration around these particles could be relieved by forming voids with very little or no deformation as indicated by their round shape. Eventual coalescence of these voids leads to loss of adhesion between the oxide and boat and in turn spallation of the top coat. Evidently, the higher concentration of Ti in alloy 1 would be expected to accelerate the above process, which could explain the observed difference in coating performance on the two alloys.

4 Conclusion

Based upon the results of this study, it could be concluded that the presence of Ti in superalloy substrates could significantly influence the useful life of thermal barrier coating systems used in gas turbine blade applications. This effect was correlated with forming Ti-rich oxide particles near the bond coat surface degrading the adherence of the thermally grown oxide. However, the
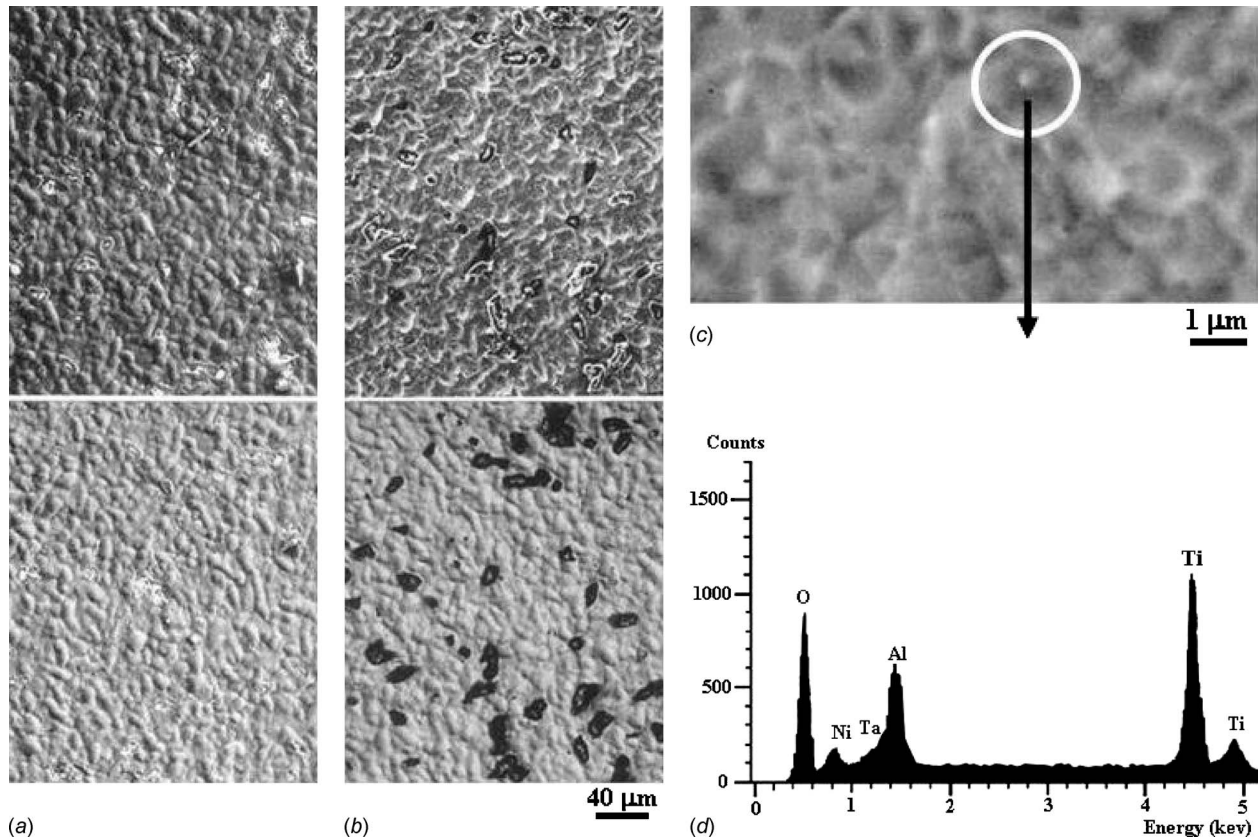
Fig. 8 An example derived from alloy 1 to illustrate typical microstructural features of the surfaces exposed by failure of the coating system (288 h of exposure at 1150°C): (*a*) exposed surface of the top coat (top: secondary electron image, bottom: backscattered image), (*b*) exposed surface of the bond coat (top: secondary electron image, bottom: backscattered image), (*c*) secondary electron image of the exposed surface of bond coat showing voids containing Ti-rich oxide particles, and (*d*) an energy dispersive X-ray spectrum showing the composition of the particle in (c) as indicated by the arrow
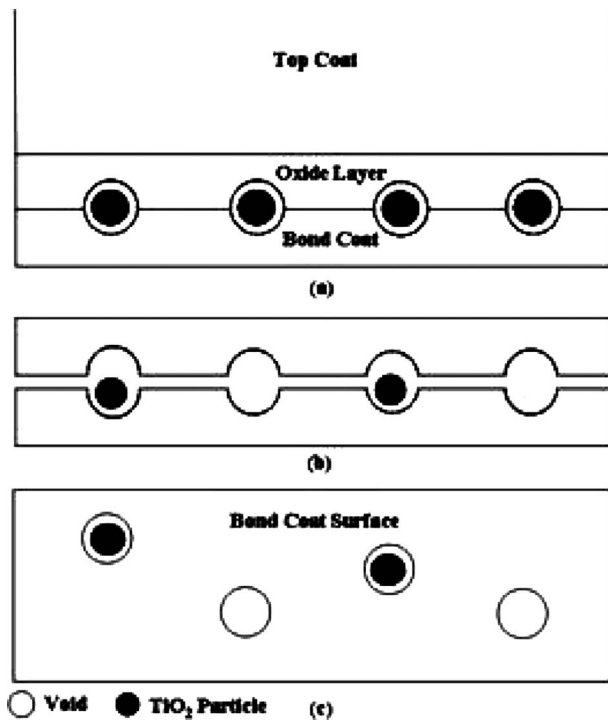
Fig. 9 Schematics illustrating possible sequence of events leading to loss of adhesion between the thermally grown oxide and bond coat by formation of Ti-rich oxide particles near the oxide-bond coat interface: (*a*) formation of voids around oxide particles, (*b*) coalescence of voids, and (*c*) morphology of the exposed surface of bond consistent with the image of Fig. 8(*c*)

Ti-effect appeared to be critically dependent on the exact concentration. Within the limitation of this study, the effect appeared to become more pronounced at relatively high concentrations of about 1 wt %.

References

[1] Evans, A. G., Mumm, D. R., Hutchinson, J. W., Meier, G. H., and Petit, F. S., 2001, "Mechanisms Controlling the Durability of Thermal Barrier Coatings," Prog. Mater. Sci., **46**, pp. 505–553.

[2] Smialek, J. L., and Meier, G. H., 1987, *Superalloys II*, C. T. Sims, N. S. Stoloff, and W. C. Hagel, eds., Wiley, New York, pp. 293–326.

[3] Levy, M., Farrell, P., and Pettit, F., 1986, "Oxidation of Some Advanced Single-Crystal Nickel-Base Superalloys in Ait at 2000 F (1093 °C)," Corrosion-NACE, **42**(12), pp. 708–717.

[4] Tawancy, H. M., and Al-Hadhrami, L. M., 2010, "Role of Platinum in Thermal Barrier Coatings Used in Gas Turbine Blade Applications," ASME J. Eng. Gas Turbines Power, **132**(2), p. 022103.

[5] Tawancy, H. M., UI-Hamid, A., Aboelfotoh, M.O., and Abbas, N. M., 2008, "Effect of Pt on the Oxide-to-Metal Adhesion in Thermal Barrier Coatings," J. Mater. Sci., **43**(9), pp. 2978–2989.

[6] Zhang, Y., Stacy, J. P., Pint, B. A., Haynes, J. A., Hazel, B.T., and Nagaraj, B.A., 2008, "Interdiffusion Behavior of Pt-Diffused $\gamma+\gamma'$ Coatings on Ni-Based Alloys," Surf. Coat. Technol., **203**, pp. 417–421.

[7] Zhang, Y., Pint, B. A., Haynes, J. A., and Wright, I. G., 2005, "A Platinum-Enriched $\gamma+\gamma'$ Two-Phase Bond Coat on Nickel-Based Superalloys," Surf. Coat. Technol., **200**(5–6), pp. 1259–1263.

[8] Gleeson, B., Mu, N., and Hayashi, S., 2009, "Compositional Factors Affecting the Establishment and Maintenance of Al_2O_3 Scales on Ni–Al–Pt Systems," J. Mater. Sci., **44**, pp. 1704–1710.

[9] Hayashi, S., Wang, W., Sordelet, D. J., and Gleeson, B., 2005, "Interdiffusion Behavior of Pt-Modified Gamma-Ni+Gamma′-Ni3Al Alloys Coupled to Ni–Al-Based Alloys," Metall. Mater. Trans. A, **36A**(7), pp. 1669–1775.

[10] Hayashi, S., Ford, S. I., Young, D. J., Sordelet, D. J., Besser, M. F., and Gleeson, B., 2005, "α-NiPt(Al) and Phase Equilibria in the Ni–Al–Pt System at 1150 °C ," Acta Mater., **53**(11), pp. 3319–3328.

[11] Lammermannm, H., and Kienel, G., 1991, "PVD Coatings for Aircraft Turbine Blades," Advanced Materials and Processes, **140**(6), pp. 18–23.

[12] Douglas, A., Hill, P. J., Murakumo, T., Cornish, L. A., and Suss, R., 2009, "The Platinum Development Initiative: Platinum Based Alloys for High Temperature and Special Applications: Part II," Platinum Met. Rev., **53**(2), pp. 69–77.

[13] Cornish, L. A., Suss, R., Watson, A., and Prins, S. N., 2007, "Building a Thermodynamic Database for Platinum-Based Superalloys: Part I," Platinum Met. Rev., **51**(3), pp. 104–115.